International Journal of Non-Linear Mechanics 129 (2021) 103653

Contents lists available at ScienceDirect

International Journal of Non-Linear Mechanics

journal homepage: www.elsevier.com/locate/nlm

Uncertainty analysis of heart dynamics using Random Matrix Theory

Augusto Cheffer, Thiago G. Ritto, Marcelo A. Savi *

Center for Nonlinear Mechanics, COPPE – Department of Mechanical Engineering, Universidade Federal do Rio de Janeiro, 21.941.972 – Rio de Janeiro – RJ, P.O. Box 68.503, Brazil

ARTICLE INFO

Keywords:
Nonlinear dynamics
Chaos
Cardiac rhythms
DDEs
Random matrix theory

ABSTRACT

This paper deals with the uncertainty analysis of the cardiac system described by a mathematical model. The model is composed of three-coupled nonlinear oscillators with time-delayed connections. The main idea is to investigate heart dynamics using the Random Matrix Theory, modeling uncertainties and establishing the impact of the probabilistic model on the dynamic response of the system Two advantages of the proposed methodology should be pointed out: model uncertainties are taken into account considering, for instance, connection among different oscillators; and the uncertainty level is controlled by only one parameter. Results show that, in general, the model is able to capture the main dynamic behaviors of the cardiac system. It is also observed that pathological behaviors can evolve from normal rhythms due to random couplings.

1. Introduction

A representative and widespread signal of cardiac rhythm is the electrocardiogram (ECG) that records the heart electrical activity in the form of waves. It is possible to represent the electrical current in different areas of the heart allowing a comprehension about heart rhythms, elucidating the difference between normal or pathological signals.

The human heart is divided into 4 cavities: 2 atria and 2 ventricles (Fig. 1a). The conduction of the electrical impulse in the cardiac system can be understood as a network of self-excitatory elements formed by sinoatrial node (SA), atrioventricular node (AV) and His–Purkinje complex (HP) ([1,2]). The initial excitation occurs in the SA node, natural pacemaker, and propagates as a wave, stimulating atria. Upon reaching the AV node, it initiates a pulse that excites the bundle of His and, afterward, the Purkinje fibers. The fibers distribute the stimulus to the myocardial cells, causing the ventricles contraction [3]. Fig. 1b presents a schematic picture of a normal cardiac cycle, showing the main waves: P wave that represents the impulse generated by the SA node; the QRS complex that is formed by ventricular contraction; and the T wave that reflects ventricular repolarization. In addition, it should be pointed out an important characteristic of the ECG, the RR interval that can vary in an apparently regular behavior.

A relevant analysis from ECGs is the based on instantaneous heart rate variations using RR interval time series to define the so-called heart rate variability (HRV) [4], which can be considered one of the best predictors of arrhythmic events [5]. Unavoidable noise contamination demands reliable signal processing techniques and, among them, it is important to cite the detection of R-peaks ([6,7]) and calculation of heart and breathing rate variability [4,8]. HRV can be considerably different even in the absence of physical or mental stress and this information has been applied for clinical and research purposes. The existence of HRV points that, besides nonlinear characteristics, heart system can present some random behavior.

Deterministic chaos and random noise of the heart rhythm analysis are compared by Kantz and Schreiber [9]. Bozóki [10] developed a data acquisition method for fetal heart rate suitable to be used by both power spectral analysis (statistical) and chaos theory (deterministic). An analysis of canine ECGs made by Kaplan and Cohen [7] suggested that fibrillation is similar to a random signal. It is also shown that a deterministic dynamical system can generate random-looking, non-chaotic behavior. The challenges to make decision between determinist or statistical analysis to treat human cardiovascular behavior are presented by Yates and Benton [11]. Deng et al. [12] presented an ECG identification framework via deterministic dynamic neural learning mechanism for human cardiac pattern classification. According to a symbolic analysis in atrial fibrillation surrogate data made by Aronis et al. [13], pathological response is not driven by a rescaled linear stochastic process or a fractional noise. They supported the development of deterministic or nonlinear stochastic modeling. Son et al. [14] developed a stochastic cardiovascular-pump model representing the effects of left ventricular assist devices on heart hemodynamics. Based on these references, it is possible to conclude that deterministic and random aspects are important for the comprehension of heart system dynamics.

An alternative for the heart dynamics analysis is the consideration of mathematical models. Grudzinski and Zebrowski [15] proposed

* Corresponding author.
E-mail addresses: augusto.cheffer@poli.ufrj.br (A. Cheffer), tritto@mecanica.ufrj.br (T.G. Ritto), savi@mecanica.coppe.ufrj.br (M.A. Savi).

https://doi.org/10.1016/j.ijnonlinmec.2020.103653
Received 6 May 2020; Received in revised form 30 September 2020; Accepted 26 November 2020
Available online 28 November 2020

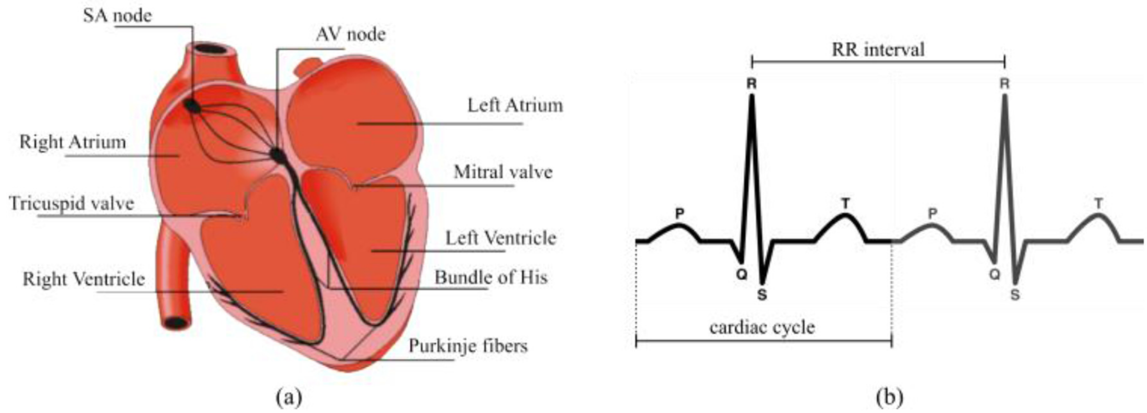

Fig. 1. Human heart. (a) Anatomy of the heart. (b) Schematic ECG response representing a normal cardiac cycle.

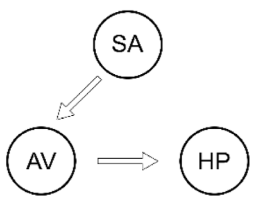

Fig. 2. Conceptual model of the normal heart functioning.

modifications on the original Van der Pol oscillator in order to present a more suitable description of the natural pacemaker. Dos Santos et al. [16] presented a simplified cardiac system model considering two asymmetrically coupled modified Van der Pol oscillators, representing the behavior of the two cardiac pacemakers, SA and AV nodules. Gois and Savi [1] proposed a three-coupled oscillator model in order to represent ECG signals. Besides, SA and AV nodules, HP complex is also considered in system modeling. Each oscillator is based on the model due to Grudzinski and Zebrowski [15] and the system has bidirectional and asymmetric time-delayed couplings to represent the time spent on impulse transmissions. Cheffer and Savi [17] improved the three-coupled oscillator model proposed by Gois and Savi [1] and introduced random connections among oscillators. Basically, results pointed that the combination of nonlinearities and randomness can provide a great variety of possibilities of the heart dynamics. Jawarneh and Staffeldt [18] developed a study of bifurcations on a modified van der Pol oscillator applying Conley index methods. Cardarilli et al. [19] proposed a model with four modified Van der Pol oscillators representing the groups: SA and AV nodes, Right and Left bundle branches. This model is based on Fitz-Hugh–Nagumo equations [20] and is motivated as an improvement to simulate branch blocks.

Concerning stochastic modeling, several approaches can be applied for uncertainty quantification. Probabilistic approach is widely used in structural dynamics [21]. In this regard, the parametric probabilistic approach considers uncertainties in the model parameters, and therefore, a probabilistic model is constructed to each parameter of the system. On the other hand, nonparametric probabilistic approach [22] considers uncertainties in the model itself, and probabilistic model is constructed directly for the generalized matrices of the system. The rationale behind the idea of considering Random Matrix Theory (RMT) to take into account model uncertainties can be found in [22] and [23]. A historical review of the Random Matrix Theory can be found in [24].

Uncertainties in heart dynamics are treated in some research efforts. Christini et al. [25] found similar levels of spectral uncertainties for both experimental heart rate data and synthetic autoregressive time

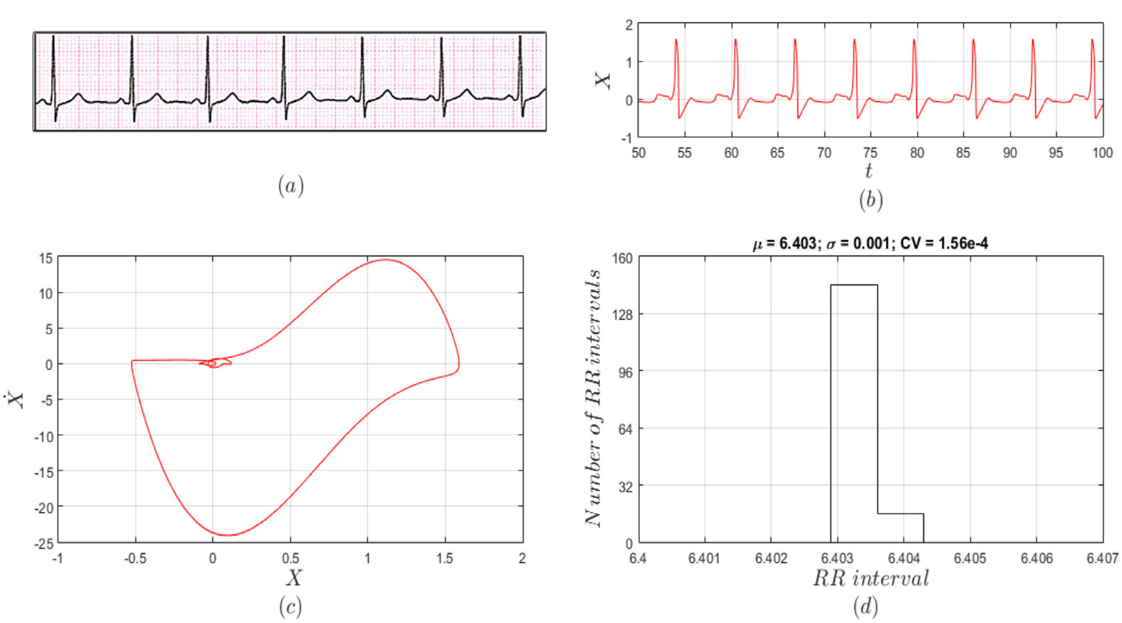

Fig. 3. Normal ECG. (a) Experimental (physionet.org) and simulated response: (b) times series, (c) phase plane and (d) RR histogram.

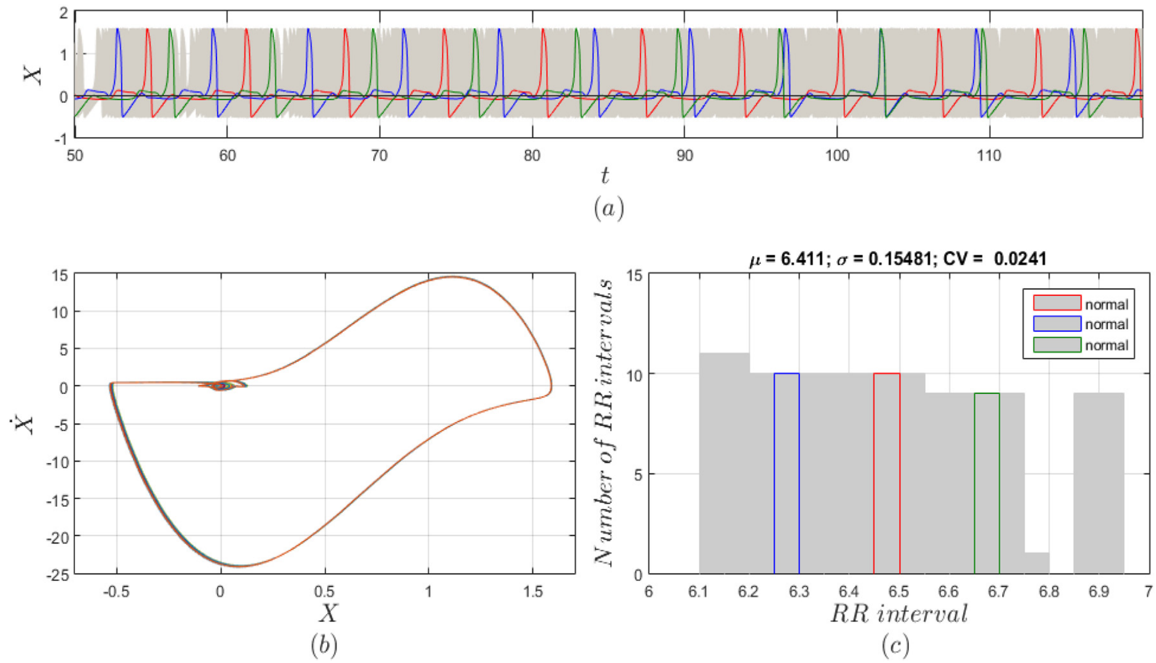

Fig. 4. Stochastic analysis of $\boldsymbol{K}_{BD}$ with $\sigma_M = 0.01$: (a) ECG Monte Carlo response samples; (b) respective state spaces and (c) RR histograms.

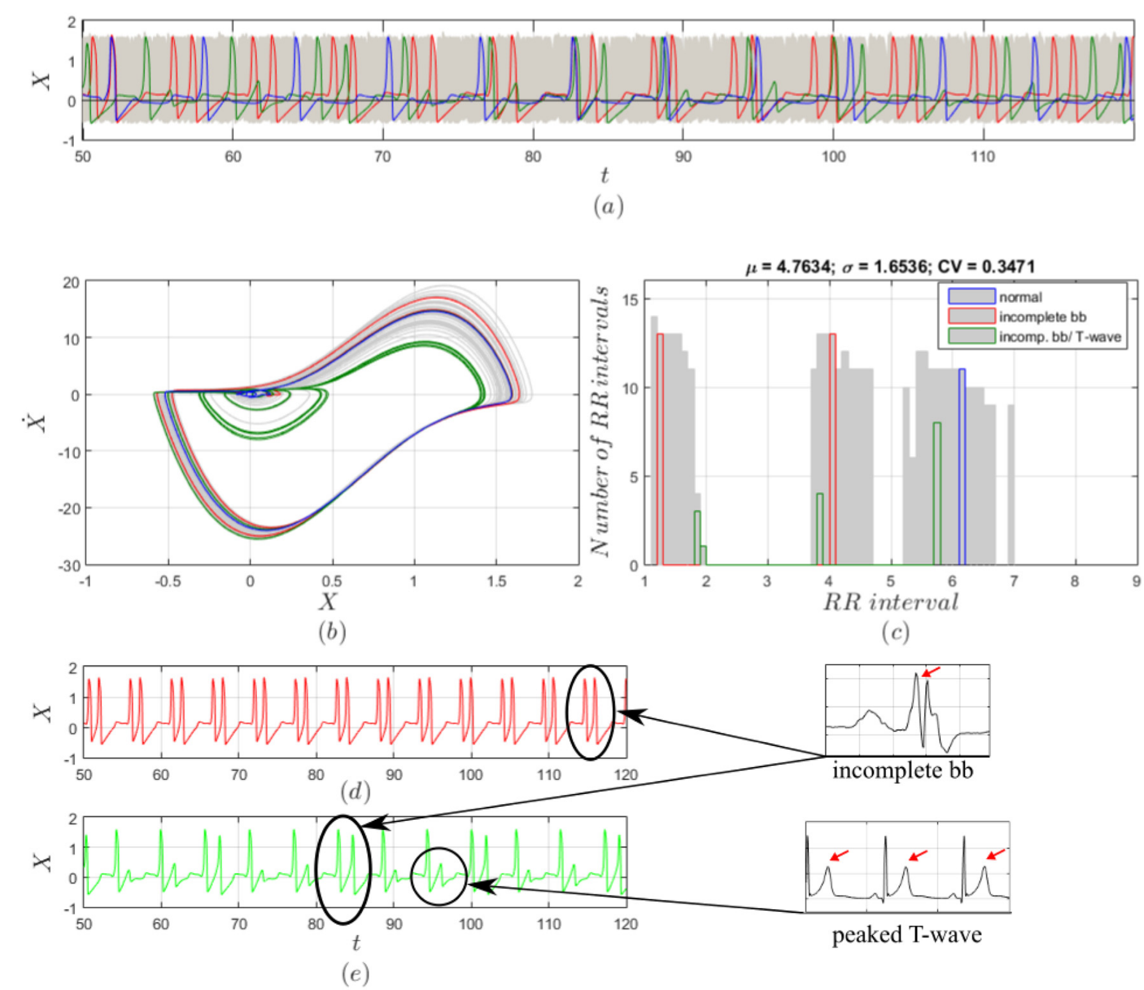

Fig. 5. Stochastic analysis of $\boldsymbol{K}_{BD}$ with $\sigma_M = 0.1$: (a) ECG Monte Carlo response samples; (b) respective state spaces and (c) RR histograms. (d) Incomplete bb and (e) incomplete bb with variable T-wave . (For interpretation of the references to color in this figure legend, the reader is referred to the web version of this article.)

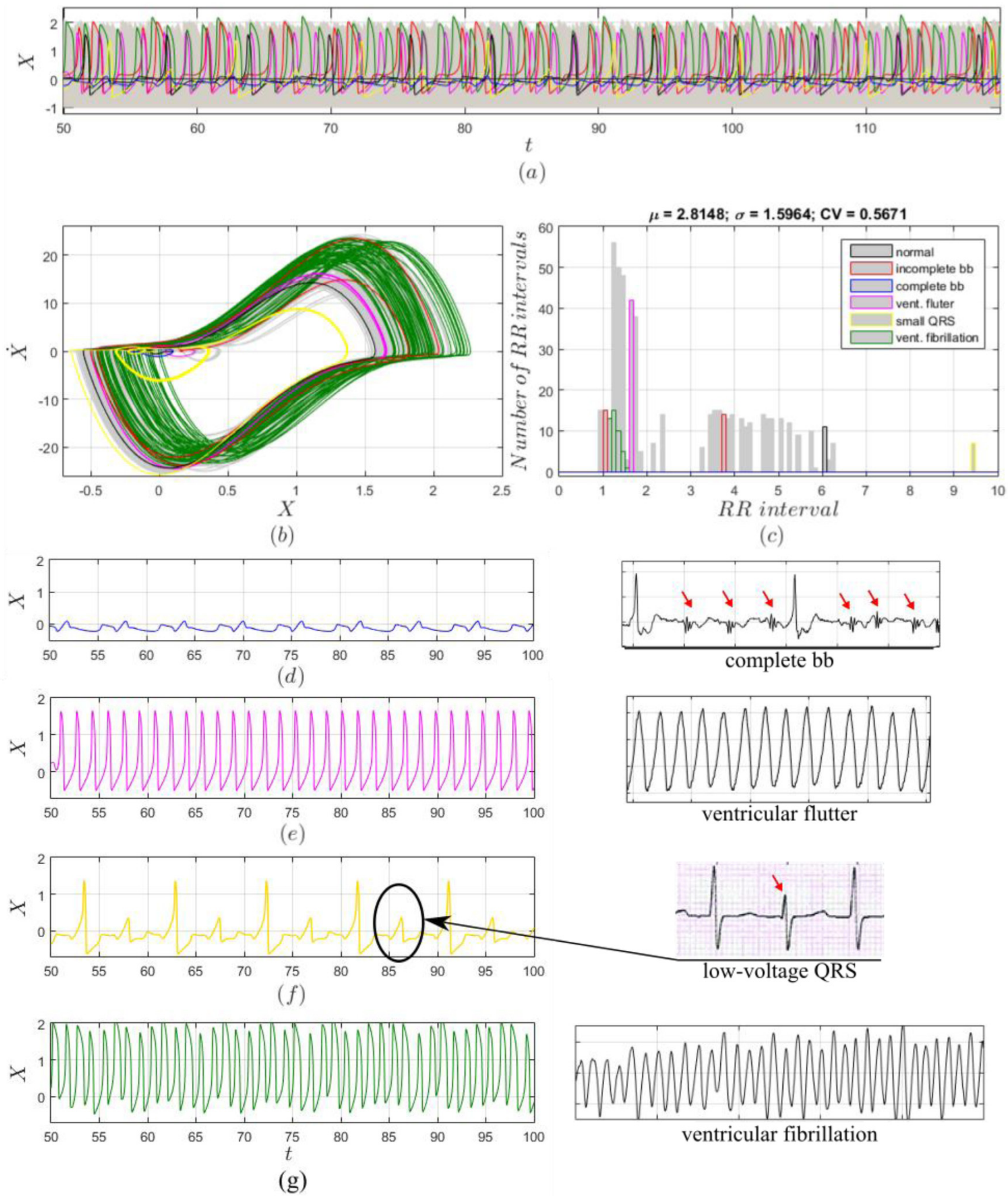

Fig. 6. Stochastic analysis of $\boldsymbol{K}_{BD}$ with $\sigma_M = 1.0$: (a) ECG Monte Carlo response samples; (b) respective state spaces and (c) RR histograms. (d) Complete bb, (e) ventricular flutter, (f) low-voltage QRS and (g) ventricular fibrillation type 1 . (For interpretation of the references to color in this figure legend, the reader is referred to the web version of this article.)

series by applying Monte Carlo analysis. Johnstone et al. [26] discussed uncertainty quantification in cardiac action potential models and experimental canine action potential models. Pathmanathan et al. [27] presented a novel action potential model that includes input variability for all parameters and performed uncertainty quantification and sensitivity analysis for a range of behaviors with physiological relevance.

This work deals with a probabilistic approach that relies on RMT [28] and Gaussian Orthogonal Ensemble (GOE) [23,29] to describe uncertainties of the cardiac system. Random matrices have been used to represent model inadequacy, for instance, in the context of chemical kinetics [30], and in voice signals with pathologies [31].

The main idea of the present work is to use the mathematical description proposed by Gois and Savi [1] and introduce random matrices to describe uncertainties in some operators, that introduce coupling terms that were not there before. Under this assumption, the cardiac system is described by a system of delayed differential equations that represents three oscillators connected by delayed and random terms. Model uncertainties are taken into account considering only one parameter that controls the uncertainty level. This is a special advantage since the alternative strategy is to consider individually, eighteen uncertain coupling parameters. Different kinds of connections are evaluated establishing situations where pathological behaviors evolve from normal rhythm due to random aspects.

The paper is organized as follows. A mathematical model is proposed in terms of matrix blocks in order to use the random matrix theory in Section 2. Afterward, numerical simulations are developed

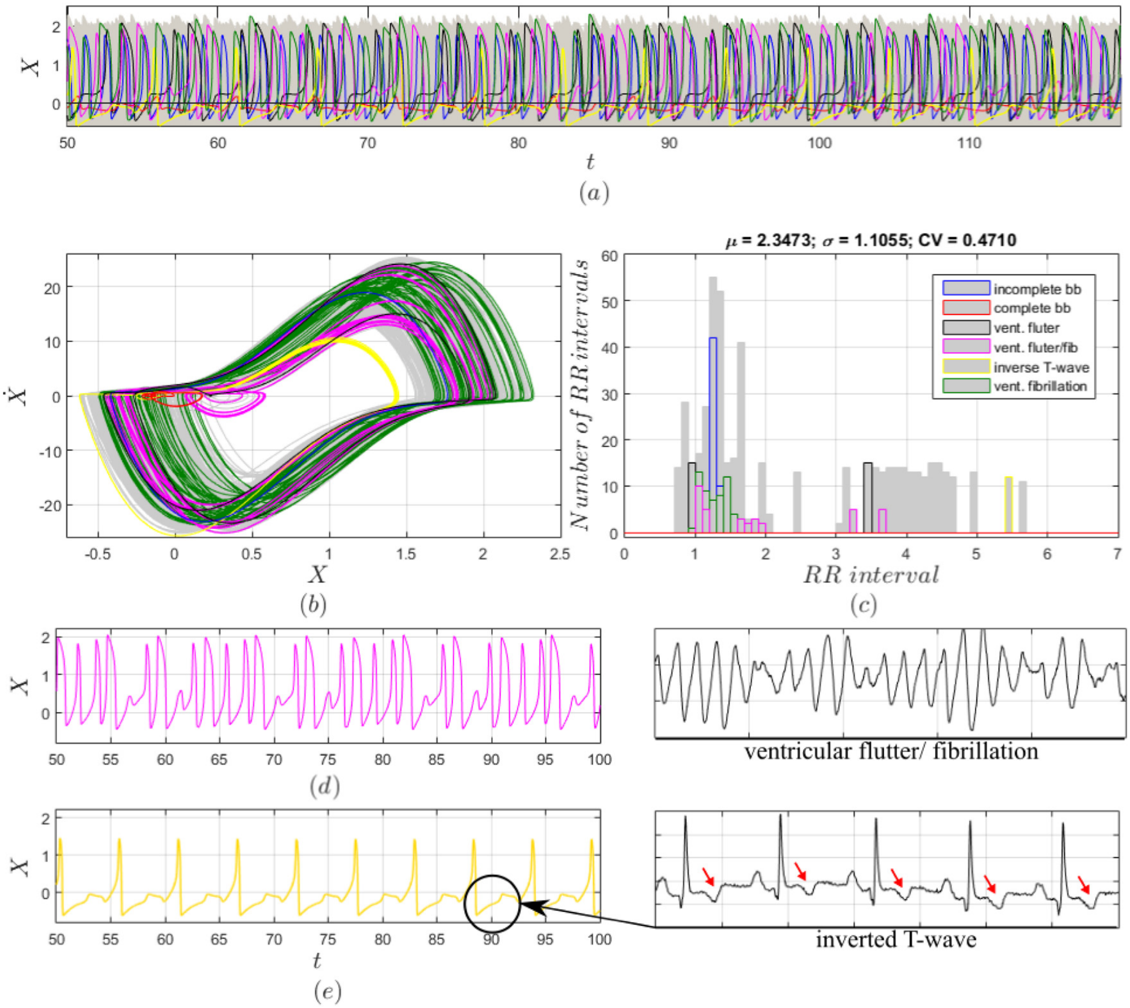

Fig. 7. Stochastic analysis of $\boldsymbol{K}_{BD}$ with $\sigma_M = 3.0$: (a) ECG Monte Carlo response samples; (b) respective state spaces and (c) RR histograms. (d) Ventricular flutter and fibrillation combination and (e) inverted T-wave . (For interpretation of the references to color in this figure legend, the reader is referred to the web version of this article.)

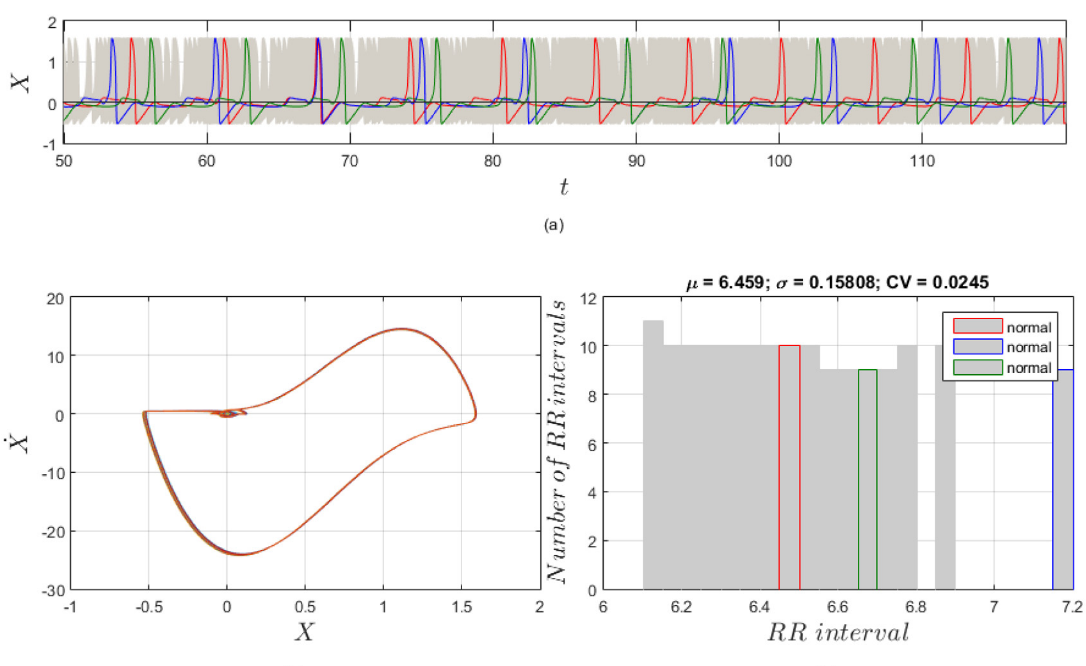

Fig. 8. Stochastic analysis of $\boldsymbol{K}_{BI}$ with $\sigma_M = 0.01$: (a) ECG Monte Carlo response samples; (b) respective state spaces and (c) RR histograms.

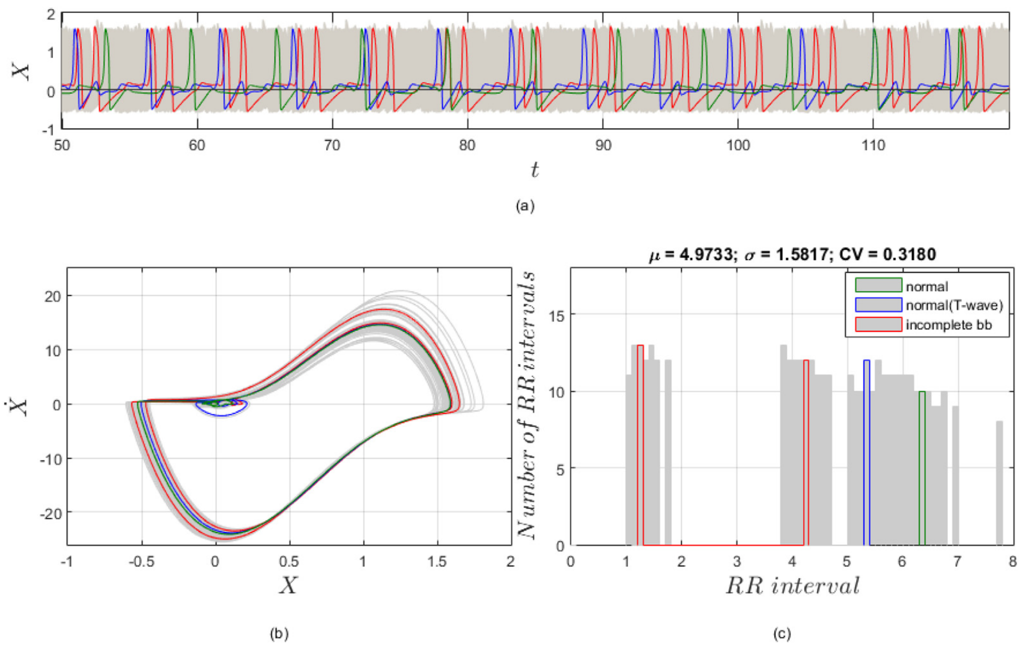

Fig. 9. Stochastic analysis of $\boldsymbol{K}_{BI}$ with $\sigma_M = 0.1$: (a) ECG Monte Carlo response samples; (b) respective state spaces and (c) RR histograms . (For interpretation of the references to color in this figure legend, the reader is referred to the web version of this article.)

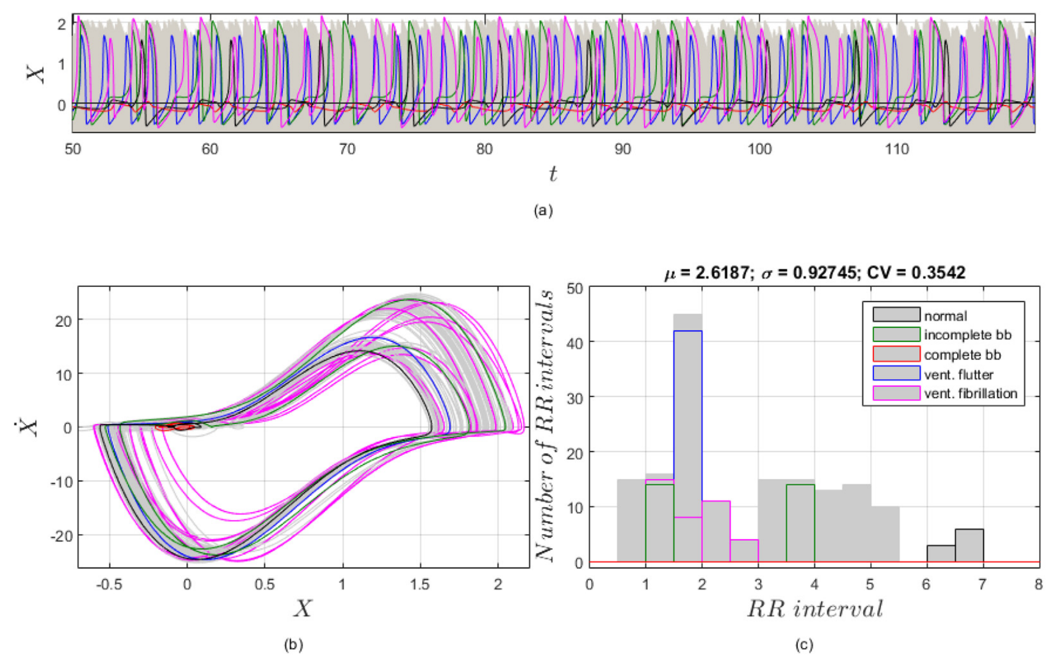

Fig. 10. Stochastic analysis of $\boldsymbol{K}_{BI}$ with $\sigma_M = 1.0$: (a) ECG Monte Carlo response samples; (b) respective state spaces and (c) RR histograms . (For interpretation of the references to color in this figure legend, the reader is referred to the web version of this article.)

showing some heart behaviors, highlighting their aspects on ECG and state space. Final remarks are presented in the sequence.

2. Mathematical model

A mathematical model to describe heart dynamics can be formulated considering three coupled nonlinear oscillators that represent the electrical behavior of the sino-atrial (SA) node, the atrio-ventricular (AV) node, and the His–Purkinje complex (HP). SA node is the natural cardiac pacemaker, while AV node is a secondary pacemaker. Each oscillator is based on the model due to Grudzinski and Zebrowski [15] and the system has bidirectional and asymmetric time-delayed couplings to represent the time spent on impulse transmissions. In this regard, the governing equations can be written in matrix form as follows [17]:

$$\dot{\boldsymbol{x}} = \boldsymbol{H}(\boldsymbol{x}) + \boldsymbol{F}(t) + \boldsymbol{K}\boldsymbol{x} + \boldsymbol{K}^{\tau}\boldsymbol{x}^{\tau} \tag{1}$$

where $\boldsymbol{x}$ is the state space vector; $\boldsymbol{x}^{\tau}$ is the delayed state space vector; $\boldsymbol{H}(\boldsymbol{x})$ is the system vector field; $\boldsymbol{F}(t)$ represents external stimulus; $\boldsymbol{K}$ is the coupling matrix; and $\boldsymbol{K}^{\tau}$ is the delayed coupling matrix. The definition of each one of these terms is presented in the sequence based on the original model of Cheffer and Savi [17] and Gois and Savi [1] $\boldsymbol{x}, \boldsymbol{x}^{\tau}, \boldsymbol{H}(\boldsymbol{x}), \boldsymbol{K}, \boldsymbol{K}^{\tau}$ are given in Box I,

$$\boldsymbol{x} = \begin{bmatrix} x_1 & x_3 & x_5 & x_2 & x_4 & x_6 \end{bmatrix}^{\boldsymbol{T}};$$
$$\boldsymbol{x}^{\boldsymbol{\tau}} = \begin{bmatrix} x_5^{\tau_{HP-SA}} & x_1^{\tau_{SA-AV}} & x_3^{\tau_{AV-HP}} & x_3^{\tau_{AV-SA}} & x_5^{\tau_{HP-AV}} & x_1^{\tau_{SA-HP}} \end{bmatrix}^{\boldsymbol{T}};$$
$$\boldsymbol{H}(\boldsymbol{x}) = \begin{bmatrix} x_2 \\ x_4 \\ x_6 \\ -\alpha_{SA}x_2\left(x_1 - v_{SA1}\right)\left(x_1 - v_{SA2}\right) - \dfrac{x_1(x_1+d_{SA})(x_1+e_{SA})}{d_{SA}+e_{SA}} \\ -\alpha_{AV}x_4\left(x_3 - v_{AV1}\right)\left(x_3 - v_{AV2}\right) - \dfrac{x_3(x_3+d_{AV})(x_3+e_{AV})}{d_{AV}+e_{AV}} \\ -\alpha_{HP}x_6\left(x_5 - v_{HP1}\right)\left(x_5 - v_{HP2}\right) - \dfrac{x_5(x_5+d_{HP})(x_5+e_{HP})}{d_{HP}+e_{HP}} \end{bmatrix}; \boldsymbol{F}(t) = \begin{bmatrix} 0 \\ 0 \\ 0 \\ F_{SA}(t) \\ F_{AV}(t) \\ F_{HP}(t) \end{bmatrix};$$
$$\boldsymbol{K} = \begin{bmatrix} 0 & 0 & 0 & 0 & 0 & 0 \\ 0 & 0 & 0 & 0 & 0 & 0 \\ 0 & 0 & 0 & 0 & 0 & 0 \\ -(k_{AV-SA}+k_{HP-SA}) & 0 & 0 & 0 & 0 & 0 \\ 0 & -(k_{SA-AV}+k_{HP-AV}) & 0 & 0 & 0 & 0 \\ 0 & 0 & -(k_{SA-HP}+k_{AV-HP}) & 0 & 0 & 0 \end{bmatrix};$$
$$\boldsymbol{K}^{\boldsymbol{\tau}} = \begin{bmatrix} 0 & 0 & 0 & 0 & 0 & 0 \\ 0 & 0 & 0 & 0 & 0 & 0 \\ 0 & 0 & 0 & 0 & 0 & 0 \\ k^{\tau}_{HP-SA} & 0 & 0 & k^{\tau}_{AV-SA} & 0 & 0 \\ 0 & k^{\tau}_{SA-AV} & 0 & 0 & k^{\tau}_{HP-AV} & 0 \\ 0 & 0 & k^{\tau}_{AV-HP} & 0 & 0 & k^{\tau}_{SA-HP} \end{bmatrix}.$$

Box I.

By assuming that indexes m and n represent SA, AV or HP, and $m \neq n$, the terms of the governing equations are explained: $x_i^{\tau_{m-n}} = x_i(t - \tau_{m-n})$ are delayed terms where τ_{m-n} is the time delay; k_{m-n} and k^{τ}_{m-n} are coupling coefficients between m and n nodes.

In addition, the delayed coupling term, $\boldsymbol{K}^{\boldsymbol{\tau}}$, can be split into matrix blocks as follows:

$$\boldsymbol{K}^{\boldsymbol{\tau}} = \begin{bmatrix} \boldsymbol{0} & \boldsymbol{0} \\ \boldsymbol{K_{BD}} & \boldsymbol{K_{BI}} \end{bmatrix}, \tag{2}$$

where $\boldsymbol{K_{BD}}$ and $\boldsymbol{K_{BI}}$ represent diagonal matrix blocks that can be interpreted, respectively, as direct and inverse directions of signal transmission among oscillators.

The ECG is represented by a combination of the signal of each one of the oscillators, being formed by a linear combination of the state variables given by [1].

$$X = ECG = \beta_0 + \beta_1 x_1 + \beta_2 x_3 + \beta_3 x_5, \tag{3}$$

where β_0, β_1, β_2 and β_3 are constants. Therefore,

$$\dot{X} = \frac{d}{dt}(ECG) = \beta_1 x_2 + \beta_2 x_4 + \beta_3 x_6. \tag{4}$$

The fourth order Runge–Kutta method with linear interpolation of time-delayed variables is used to integrate the system (1) [32]. In order to treat the DDEs system, it is necessary to approximate their solutions in time instants before τ_j. A Taylor series expansion is proposed [1,33].

$$x_i^{\tau} = x_i - \tau\left(\frac{x_{i+1} - x_i}{h}\right). \tag{5}$$

Model uncertainties are taken into account by randomly perturbing some operators of the system. The considered probabilistic model is based on Gaussian Orthogonal Ensemble (GOE), as employed by Ritto and Fabro [23] in the context of structural dynamic analysis. In order to preserve the symmetry, the following random germ matrix is considered:

$$\boldsymbol{G}_s = \left(\boldsymbol{G} + \boldsymbol{G}^T\right)/2 \tag{6}$$

where $\boldsymbol{G}$ is a random matrix with dimension $m{\times}m$, composed of independent and identically distributed normal random variables, with zero mean and standard deviation σ_M, algebraically $G_{ij} \sim N(0, \sigma_M^2)$. Therefore, only one parameter controls the level of uncertainty of the stochastic system.

The deterministic symmetric system matrix $\boldsymbol{X}_{det}$ is perturbed by the symmetric random matrix germ $\boldsymbol{G}_s$ yielding the symmetric random matrix $\boldsymbol{X}_S$:

$$\boldsymbol{X}_S = \boldsymbol{X}_{det} + \boldsymbol{G}_s \tag{7}$$

Note that $\boldsymbol{X}_S$ is symmetric by construction, and its mean value is $\boldsymbol{X}_{det}$. By applying the described stochastic modeling to the system matrices $\boldsymbol{K}_{BD}$ and $\boldsymbol{K}_{BI}$, uncertainties are introduced not only in the main diagonal, but also in the extra diagonal terms. Hence, it is possible to analyze effects of eighteen uncertainty elements of these matrices by varying just one parameter: the standard deviation σ_M.

3. Numerical simulations

Numerical simulations of the cardiac system are performed with the objective of presenting different system behaviors. Parameters are chosen in order to match experimental data and different cardiac rhythm are of concern. All experimental data are based on PhysioBank ATM (physionet.org). In all simulations, the following parameters [1] are used: $\beta_0 = 1$ mV, $\beta_1 = 0.06$ mV, $\beta_2 = 0.1$ mV, $\beta_3 = 0.3$ mV. A convergence analysis reveals that time steps smaller than 10^{-3} presents

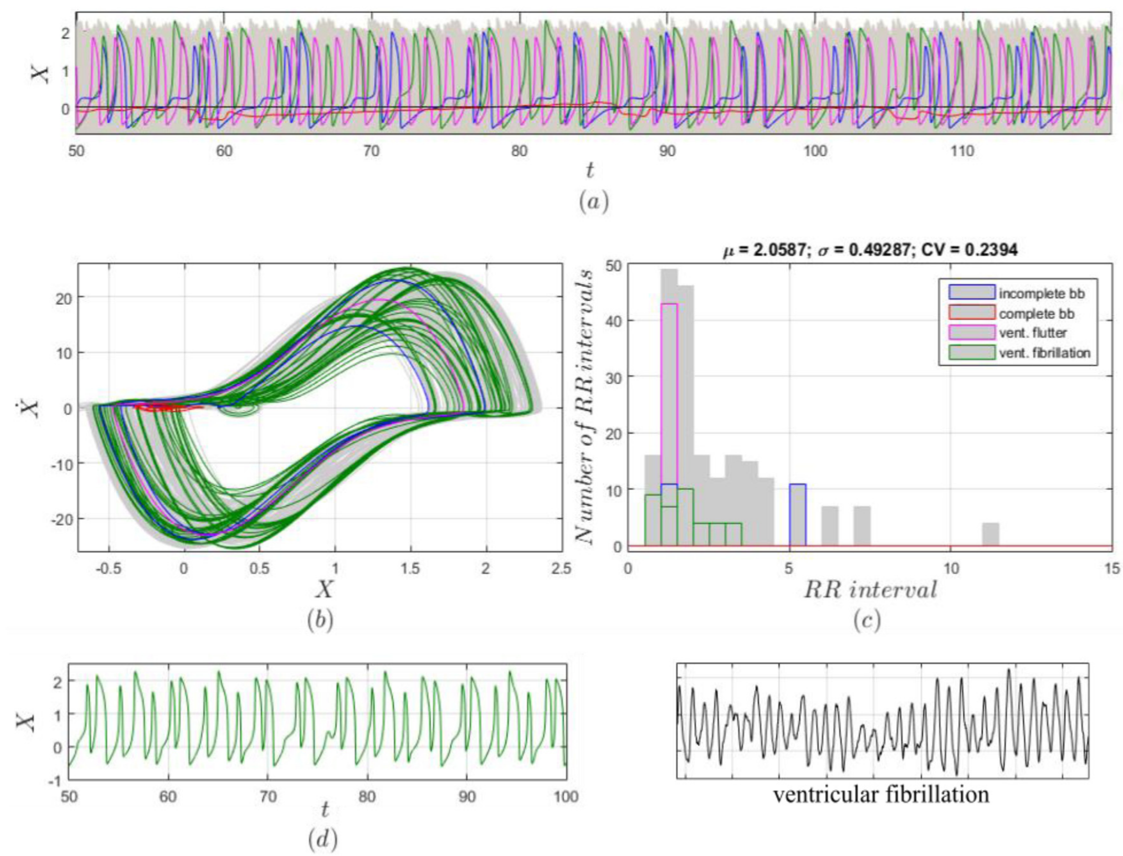

Fig. 11. Stochastic analysis of $\boldsymbol{K}_{BI}$ with $\sigma_M = 3.0$: (a) ECG Monte Carlo response samples; (b) respective state spaces and (c) RR histograms. (d) Ventricular fibrillation type 2 . (For interpretation of the references to color in this figure legend, the reader is referred to the web version of this article.)

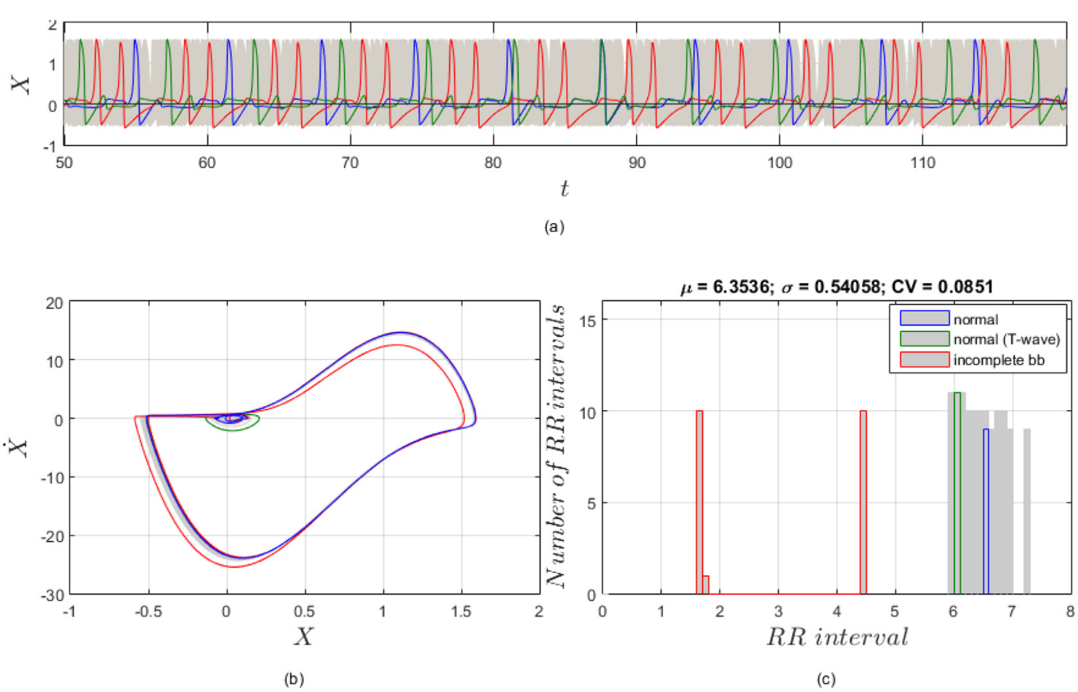

Fig. 12. Stochastic analysis of $\boldsymbol{K}_{BD}$ and $\boldsymbol{K}_{BI}$ with $\sigma_M = 0.01$: (a) ECG Monte Carlo response samples; (b) respective state spaces and (c) RR histograms . (For interpretation of the references to color in this figure legend, the reader is referred to the web version of this article.)

error of the order of 10^{-6}, considered satisfactory. The following initial conditions are applied, once again in order to match experimental data [1]:

$$x_0 = \left[-0.1 \ 0.025 \ -0.6 \ 0.1 \ -3.3 \ \frac{2}{3}\right]^T \tag{8}$$

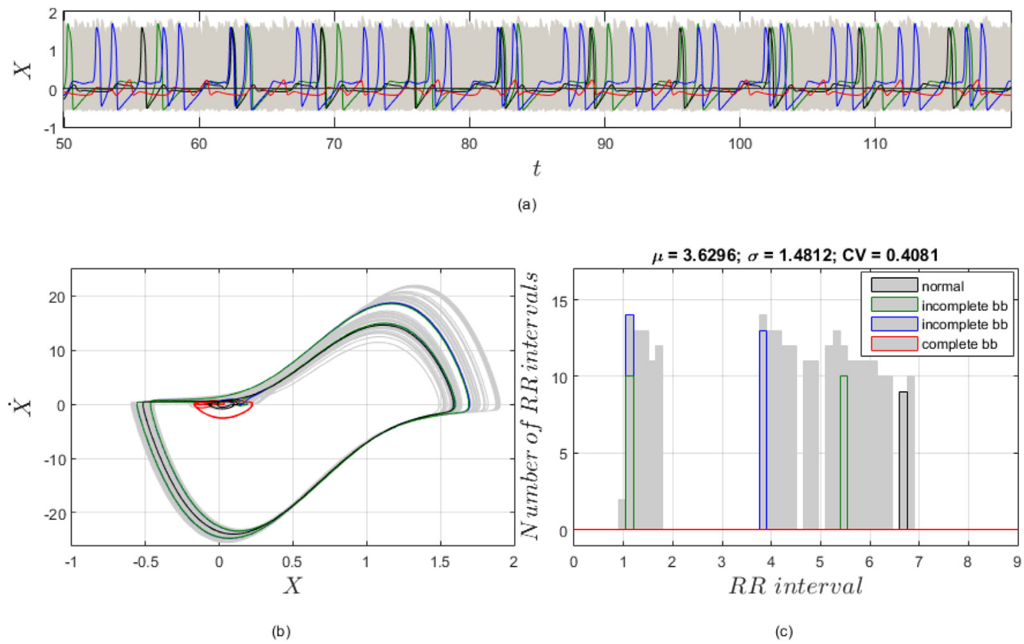

Fig. 13. Stochastic analysis of $\boldsymbol{K}_{BD}$ and $\boldsymbol{K}_{BI}$ with $\sigma_M = 0.1$: (a) ECG Monte Carlo response samples; (b) respective state spaces and (c) RR histograms . (For interpretation of the references to color in this figure legend, the reader is referred to the web version of this article.)

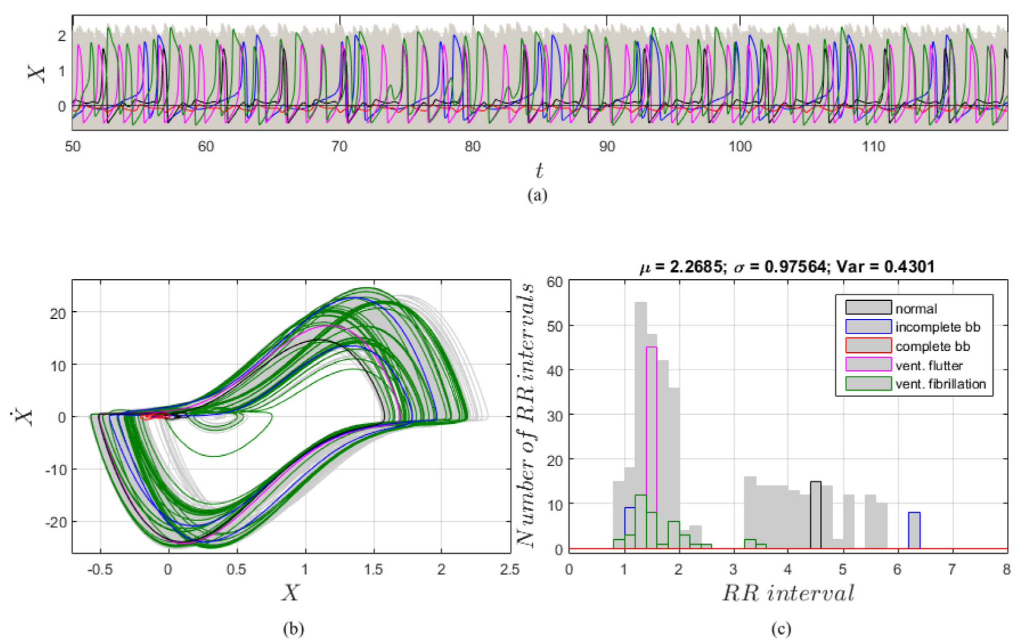

Fig. 14. Stochastic analysis of $\boldsymbol{K}_{BD}$ and $\boldsymbol{K}_{BI}$ with $\sigma_M = 1.0$: (a) ECG Monte Carlo response samples; (b) respective state spaces and (c) RR histograms . (For interpretation of the references to color in this figure legend, the reader is referred to the web version of this article.)

Normal heart rhythm has unidirectional couplings in such a way that the electrical impulse is conducted from SA node to AV node and then, from AV node to HP complex. The conceptual model of this behavior is schematically represented in Fig. 2. Table 1 shows the system parameters related to this conceptual model, vanishing all other parameters that are not presented. This means that the system does not present external stimuli. Moreover, only the couplings k_{SA-AV}, k_{AV-HP}, k^{τ}_{SA-AV} and k^{τ}_{AV-HP} and the time delays τ_{SA-AV}, τ_{AV-HP} do not vanish.

Fig. 3 presents normal rhythm and some of its representations. Fig. 3a presents an experimental ECG of normal rhythm. A simulated normal ECG is shown in Fig. 3b that captures the main features of the experimental data, presenting P, QRS and T waves. State space projection is presented in Fig. 3c showing subspace $\{X, \dot{X}\}$, from now on called phase plane. A first analysis reveals closed curves that would be associated with periodic behavior. Nevertheless, Lyapunov exponents estimation, excluding the exponent associated with time, points to null values that characterize quasi-periodic response. Fig. 3d presents a histogram of the normal rhythm RR interval showing a mean $\mu = 6.403$, and standard deviation, $\sigma = 0.001$.

Stochastic modeling is applied on $\boldsymbol{K}_{BD}$ and $\boldsymbol{K}_{BI}$ in order to investigate effects of their uncertainties, which are measured by the standard deviation σ_M, on heart model response for three cases: $\boldsymbol{K}_{BD}$ is stochastic; $\boldsymbol{K}_{BI}$ is stochastic; and both $\boldsymbol{K}_{BD}$ and $\boldsymbol{K}_{BI}$ are stochastic. This analysis is motivated by a physiology interpretation that points that some pathologies are driven by stimulus propagation in a certain

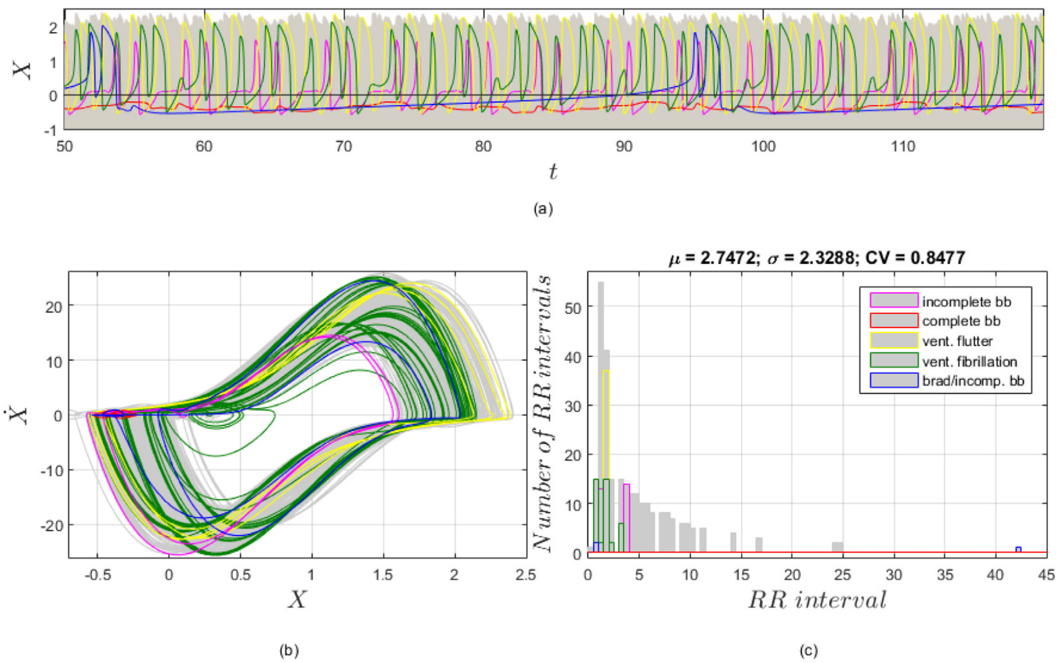

Fig. 15. Stochastic analysis of $\boldsymbol{K}_{BD}$ and $\boldsymbol{K}_{BI}$ with $\sigma_M = 3.0$: (a) ECG Monte Carlo response samples; (b) respective state spaces and (c) RR histograms . (For interpretation of the references to color in this figure legend, the reader is referred to the web version of this article.)

Table 1
Cardiac system parameters [17].

SA oscillator		HP oscillator	
α_{SA}	3	α_{HP}	7
v_{SA_1}	1	v_{HP_1}	1.65
v_{SA_2}	−1.9	v_{HP_2}	−2
d_{SA}	1.9	d_{HP}	7
e_{SA}	0.55	e_{HP}	0.67
AV oscillator		**Couplings**	
α_{AV}	3	k_{SA-AV}	3
v_{AV_1}	0.5	k_{AV-HP}	55
v_{AV_2}	−0.5	k^{τ}_{SA-AV}	3
d_{AV}	4	k^{τ}_{AV-HP}	55
e_{AV}	0.67		
		Time delays	
		τ_{SA-AV}	0.8
		τ_{AV-HP}	0.1

direction. Cheffer and Savi [17] showed that random coupling can induce different kinds of pathologies that evolve from normal rhythm. Therefore, since $\boldsymbol{K}_{BD}$ and $\boldsymbol{K}_{BI}$ represent different directions of propagation, it is reasonable to consider each matrix as random and both combined in order to represent different kinds of pathologies.

As a first approach, only diagonal terms of $\boldsymbol{G}_S$ are summed to $\boldsymbol{K}_{BD}$ and $\boldsymbol{K}_{BI}$. In this case, there is no additional coupling considered in the analysis. In order to analyze results, time series and phase plane $\{X, \dot{X}\}$ are presented. Monte Carlo simulations are employed: 100 simulations for each case and gray-shaded regions that defines the bounds of all responses are constructed. RR histograms are also constructed with Monte Carlo procedure, where 100 histograms are superimposed and each one has its mean μ_i. The mean μ, standard deviation, σ, and coefficient of variation ($CV = \frac{\sigma}{\mu}$) of this set of 100 μ_i are calculated from simulations. Convergence analysis shows that 100 simulations are enough to obtain converged behaviors of state spaces and RR histograms (including respective mean and standard deviation).

3.1. Stochastic $\boldsymbol{K}_{BD}$

Uncertainty analysis starts by considering that only $\boldsymbol{K}_{BD}$ is modeled as stochastic. Fig. 4 brings results of this analysis showing ECG, state spaces and RR histograms from Monte Carlo procedure. Note that for small values of σ_M, only normal rhythm is appearing. Time series seem desynchronized but state space shows that they are in the same orbit. RR histograms show, for each response, single peaks close to deterministic normal case. The calculated RR statistics are $\mu = 6.4110$, $\sigma = 0.1548$ and $CV = 0.0241$.

By increasing the standard deviation to $\sigma_M = 0.1$, normal, incomplete branch block (bb) rhythms and a mix of them are identified in Fig. 5. The normal response (blue) presents an orbit similar to previous case, but the RR mean is reduced, as can be seen on RR histogram. Two responses for incomplete bb are shown. One is the incomplete bb (red) characterized by double R wave and two peaks on histogram. The other one (green) is composed of incomplete bb, double R wave and T-waves with variable amplitude, generating a histogram with three peaks. Responses different from normal are highlighted in Fig. 5d (incomplete bb) and 5e (incomplete bb and variable T-wave), being compared with respective typical experimental data. In this case, RR statistics are $\mu = 4.7634$, $\sigma = 1.6536$ and $CV = 0.3471$.

Fig. 6 presents responses to $\sigma_M = 1.0$. Six rhythms can be identified: normal (black), incomplete bb (red), complete bb (blue), ventricular flutter (purple), a variation of normal with small QRS (yellow) and one type (called in this work type (1) of ventricular fibrillation (green). Besides rhythms previously described, the three new identified responses are highlighted and compared with experimental data. Complete bb (Fig. 6d) is characterized by the absence of R-waves, presenting small region loops on state space and a zero horizontal line on histogram. Ventricular flutter (Fig. 6e) is a tachycardia caused by a single ectopic focus, or peripheral reentry mechanisms, being usually caused by chronic processes (hypertensive, atherosclerotic, rheumatic), but can be induced by acute myocardial infarction. This rhythm presents state space with orbits around larger loop of normal case and one peak on RR histogram, indicating the presence of one frequency in response. The response with small QRS (Fig. 6f) exhibits state space with a closed curve with three loops: a smaller representing P and T waves, a larger referring to normal QRS and an intermediary generated by abnormal QRS. RR histogram presents a peak to the left of reference period, representing the interval between two normal QRS. Ventricular fibrillation (Fig. 6g) is a disordered myocardial contraction due to the chaotic activity of several ectopic foci located in the ventricles. This behavior results in total heart pumping inefficiency and, from the hemodynamic point of view, corresponds to cardiac arrest [34]. This rhythm presents a denser state space around the largest loop and a distribution of peaks in the interval [1, 1.7] in histogram. For this case RR statistics are $\mu = 2.8148$, $\sigma = 1.5964$ and $CV = 0.5671$.

Fig. 7 considers even a bigger standard deviation, $\sigma_M = 3.0$. Some variations of the previous responses can be identified: incomplete bb (blue), complete bb (red), ventricular flutter (black) and ventricular fibrillation (green). In addition, two new rhythms are observed: composition of ventricular flutter and fibrillation (purple, Fig. 7d) and a variation of normal with inverted T-wave (yellow, Fig. 7e). Inverted T-wave exhibits state space close to normal case but with the bigger loop a little bit smaller and one peak on RR histogram. The calculated RR statistics are $\mu = 2.3473$, $\sigma = 1.1055$ and $CV = 0.4710$.

3.2. Stochastic $\boldsymbol{K}_{BI}$

A new coupling characteristic is now of concern treating the case where $\boldsymbol{K}_{BI}$ is stochastic. Analogous to the previous case, small values of σ_M tends to be associated with normal rhythm, with a desynchronized time series and the same orbit on state space. Fig. 8 shows the system response for $\sigma_M = 0.01$ together with RR histograms that show single peaks, but with mean μ greater than previous cases with statistics $\mu = 6.4590$, $\sigma = 0.1581$ and $CV = 0.0245$.

By increasing the standard deviation to $\sigma_M = 0.1$, normal (green), a variation of normal (blue) and incomplete bb (red) are identified (Fig. 9). The variation of normal rhythm presents a T-wave with greater amplitude and can be seen on spaces states as the wider loop around $(0, 0)$. The calculated RR statistics are $\mu = 4.9733$, $\sigma = 1.5817$ and $CV = 0.3180$.

In Fig. 10 are responses for $\sigma_M = 1.0$ where it is possible to identify five rhythms: normal (black), incomplete bb (green), complete bb (red), ventricular flutter (blue) and ventricular fibrillation type 1 (purple). For this case RR statistics are $\mu = 2.6187$, $\sigma = 0.8275$ and $CV = 0.3542$.

Fig. 11 shows the case with $\sigma_M = 3.0$, presenting four kinds of response: incomplete bb (blue), complete bb (red), ventricular flutter (purple) and a different type of ventricular fibrillation (green, Fig. 11d), called here type 2. Now it exhibits different orbits also around smaller loop on spaces states and several peaks spread over a larger interval in RR histogram. Histogram statistics in this case are $\mu = 2.0587$, $\sigma = 0.4929$ and $CV = 0.2394$.

3.3. Stochastic $\boldsymbol{K}_{BD}$ and $\boldsymbol{K}_{BI}$

A general random situation is now concerned considering that both $\boldsymbol{K}_{BD}$ and $\boldsymbol{K}_{BI}$ have stochastic characteristics. Initially, a small value of standard deviation is treated $\sigma_M = 0.01$ inducing pathological responses, different from the previous cases. Fig. 12 shows three identified rhythms: normal (blue), a variation of normal with greater T-wave (green) and incomplete bb (red), whose characteristics have been already explained. The calculated RR statistics are $\mu = 6.3536$, $\sigma = 0.5406$ and $CV = 0.0851$.

By increasing the standard deviation to $\sigma_M = 0.1$, normal (black) with slightly higher RR mean, two incomplete bb (blue and green) and complete bb (red) are identified (Fig. 13). Both incomplete bb responses have double R-peaks, but with different frequencies. These results can be confirmed by different peaks location on histograms. The calculated RR statistics are $\mu = 3.6296$, $\sigma = 1.4812$ and $CV = 0.4081$.

Fig. 14 presents responses for $\sigma_M = 1.0$, showing five kinds of rhythms: normal with a lower RR mean (black), incomplete bb (blue), complete bb (red), ventricular flutter (purple) and ventricular fibrillation type 2 (green), which exhibit same response characteristics previously described. Histogram statistics are $\mu = 2.2685$, $\sigma = 0.9756$ and $CV = 0.4301$.

Fig. 15 considers a bigger standard deviation, $\sigma_M = 3.0$, showing incomplete bb (purple), complete bb (red), ventricular flutter (yellow), ventricular fibrillation type 2 (green) and a composition of incomplete bb and bradycardia (blue). The ventricular flutter now identified presents a closed curve with four loops on state space. Bradycardia designates a decrease in heart rate, which can be related to long RR interval observed on histogram. In this case RR statistics are $\mu = 2.7472$, $\sigma = 2.3288$ and $CV = 0.8477$.

4. Conclusions

A stochastic model is proposed to analyze uncertainties in a cardiac dynamical model composed of three-coupled nonlinear oscillators with time-delayed connections. The matrices related to the direct and inverse directions of signal transmission among oscillators are model as random. This strategy has the advantage of taking into account model uncertainties since it generates couplings that are not possible to obtain varying only the parameters of the system; hence, it goes beyond the usual parametric probabilistic approach. In addition, just one parameter (standard deviation) is needed to control the level of uncertainty of the system, controlling the matrix random perturbation. Monte Carlo simulations are carried out for different values of this uncertainty level parameter. The increase of the uncertainty level tends to generate signals with pathologies. Among the possible pathologies, the following cases are observed: incomplete and complete branch block (bb), bradycardia, atrial fibrillation, inverse T-wave, larger T-wave, small QRS, ventricular flutter and ventricular fibrillation. In general, it is possible to conclude that the proposed stochastic model is consistent, being able to generate cardiac pathological dynamical responses that evolve from normal rhythm.

CRediT authorship contribution statement

Augusto Cheffer: Conceptualization, Methodology, Software, Validation, Formal analysis, Investigation, Writing. **Thiago G. Ritto:** Conceptualization, Methodology, Software, Validation, Formal analysis, Investigation, Writing, Supervision, Writing - reviewing. **Marcelo A. Savi:** Conceptualization, Methodology, Software, Validation, Formal analysis, Investigation, Writing, Supervision, Writing - reviewing.

Declaration of competing interest

The authors declare that they have no known competing financial interests or personal relationships that could have appeared to influence the work reported in this paper.

Acknowledgments

The authors would like to acknowledge the support of the Brazilian Research Agencies CNPq, CAPES (Grant PROEX 803/2018) and FAPERJ.

References

[1] S.R.S.M. Gois, M.A. Savi, An analysis of heart rhythm dynamics using a three-coupled oscillator model, Chaos Solitons Fractals 41 (5) (2009) 2553–2565.

[2] L. Glass, Introduction to controversial topics in nonlinear science: Is the normal heart rate chaotic? Chaos. Interdiscip. J. Nonlinear Sci. 19 (2) (2009).

[3] D. Dubin, Interpretação rápida do ECG, Editora de Publicações Biomédicas – EPUB, Rio de Janeiro, 1996.

[4] M. Malik, A.J. Camm, Heart Rate Variability, Futura, Armonk, NY, 1995.

[5] P. Mansier, J. Clairambault, N. Charlotte, C. Médigue, C. Vermeiren, G. Lepape, F. Carré, A. Gounaropoulou, B. Swynghedauw, Linear and non-linear analyses of heart rate variability: a minireview, Cardiovasc. Res. 31 (3) (1996) 371–379.

[6] J. Pan, W.J. Tompkins, A real-time QRS detection algorithm, IEEE Trans. Biomed. Eng. BME-32 (1985) 220–236.

[7] D.T. Kaplan, R.J. Cohen, Is fibrillation chaos? Circ. Res. 67 (4) (1990) 886–892.

[8] G.B. Moody, R.G. Mark, A. Zoccola, S. Mantero, Derivation of respiratory signals from multi-lead ECGs, Comput. Cardiol. 12 (1985) (1985) 113–116.

[9] H. Kantz, T. Schreiber, Nonlinear Time Series Analysis, Ser. 7, Cambridge Nonlinear Science, USA, 2002.

[10] Z. Bozóki, Chaos theory and power spectrum analysis in computerized cardiotocography, Eur. J. Obstet. Gynecol. Reprod. Biol. 71 (2) (1997) 163–168.

[11] F.E. Yates, L.A. Benton, Variance structure in the human cardiovascular system—periodicity, chaos, or old-fashioned noise? Math. Comput. Modelling 19 (6–8) (1994) 161–170.

[12] M. Deng, C. Wang, M. Tang, T. Zheng, Extracting cardiac dynamics within ECG signal for human identification and cardiovascular diseases classification, Neural Netw. 100 (2018) 70–83.

[13] K.N. Aronis, R.D. Berger, H. Calkins, J. Chrispin, J.E. Marine, D.D. Spragg, S. Tao, H. Tandri, H. Ashikaga, Is human atrial fibrillation stochastic or deterministic? – Insights from missing ordinal patterns and causal entropy-complexity plane analysis, Chaos 28 (6) (2018) 063130, 2018.

[14] J. Son, D. Du, Y. Du, Stochastic modeling and dynamic analysis of the cardiovascular system with rotary left ventricular assist devices, Math. Probl. Eng. (2019).

[15] K. Grudzinski, J.J. Zebrowski, Modeling Cardiac Pacemakers with relaxation oscillators, Physica A 336 (2004) 153–162.

[16] A.M. Dos Santos, S.R. Lopes, R.R.L. Viana, Rhythm synchronization and chaotic modulation of coupled Van der Pol oscillators in a model for the heartbeat, Phys. A. Stat. Mech. App. 338 (3) (2004) 335–355.

[17] A. Cheffer, M.A. Savi, Random effects inducing heart pathological dynamics: An approach based on mathematical models, Biosystems (2020) 104–177.

[18] I. Jawarneh, R. Staffeldt, Conley Index Methods Detecting Bifurcations in a Modified van der Pol Oscillator Appearing in Heart Action Models, Vol. 1901, arXiv, 2019, p. 11180.

[19] G.C. Cardarilli, L. Di Nunzio, R. Fazzolari, M. Re, F. Silvestri, Improvement of the cardiac oscillator based model for the simulation of bundle branch blocks, Appl. Sci. 9 (18) (2019) 3653.

[20] E. Ryzhii, M. Ryzhii, Modeling of heartbeat dynamics with a system of coupled nonlinear oscillators, in: International Conference on Biomedical Informatics and Technology, 2013, pp. 67–75.

[21] E.T. Jaynes, Probability Theory: The Logic of Science, Cambridge University Press, 2003.

[22] C. Soize, A nonparametric model of random uncertainties for reduced matrix models in structural dynamics, Probab. Eng. Mech. 15 (3) (2000) 277–294.

[23] T.G. Ritto, A.T. Fabro, Investigation of random matrix applications on structural dynamics using a tensor decomposition, J. Braz. Soc. Mech. Sci. Eng. 41 (8) (2019) 352.

[24] P.J. Forrester, N.C. Snaith, J.J.M. Verbaarschot, Developments in random matrix theory, J. Phys. A: Math. Gen. 36 (2003) 12.

[25] D.J. Christini, A. Kulkarni, S. Rao, E.R. Stutman, F.M. Bennett, J.M. Hausdorff, N. Oriol, K.R. Lutchen, Influence of autoregressive model parameter uncertainty on spectral estimates of heart rate dynamics, Ann. Biomed. Eng. 23 (2) (1995) 127–134.

[26] R.H. Johnstone, E.T. Chang, R. Bardenet, T.P. De Boer, D.J. Gavaghan, P. Pathmanathan, R.H. Clayton, G.R. Mirams, Uncertainty and variability in models of the cardiac action potential: Can we build trustworthy models? J. Mol. Cell. Cardiol. 96 (2016) 49–62.

[27] P. Pathmanathan, J.P. Cordeiro, R.A. Gray, Comprehensive uncertainty quantification and sensitivity analysis for cardiac action potential models, Front. Physiol. 10 (2019).

[28] M.L. Mehta, Random Matrices, Revised and Enlarged, second ed., Academic Press, New York, USA, 1991.

[29] R.L. Weaver, Spectral statistics in elastodynamics, J. Acoust. Soc. Am. 85 (3) (1989) 1005–1013.

[30] R.E. Morrison, T.A. Oliver, R.D. Moser, Representing model inadequacy: A stochastic operator approach, SIAM/ASA J. Uncertain. Quantif. 6 (2) (2018) 457–496.

[31] E. Cataldo, C. Soize, Jitter generation in voice signals produced by a two-mass stochastic mechanical model, Biomed. Signal Process. Control 27 (2016) 87–95.

[32] B. Mensour, A. Longtin, Power spectra and dynamical invariants for delay-differential and difference equations, Physica D 113 (1) (1998) 1–25.

[33] W.J. Cunningham, A nonlinear differential-difference equation of growth, Proc. Natl. Acad. Sci. 40 (8) (1954) 708–713.

[34] G.J. Klein, T.M. Bashore, T.D. Sellers, E.L. Pritchett, W.M. Smith, J.J. Gallagher, Ventricular fibrillation in the Wolff-Parkinson-White syndrome, New Engl. J. Med. 301 (20) (1979) 1080–1085.